

Electronic Structure, Phonons and Dielectric Anomaly in Ferromagnetic Insulating Double Perovskite $\text{La}_2\text{NiMnO}_6$

Hena Das¹, Umesh V. Waghmare², T. Saha-Dasgupta^{*,1} and D. D. Sarma^{3,4}

¹ *Satyandranath Bose National Centre for Basic Sciences, Kolkata 700098, India*

² *Jawaharlal Nehru Centre for Advanced Scientific Research, Jakkur, Bangalore 560064, India*

³ *Centre for Advanced Materials, Indian Association for the Cultivation of Science, Jadavpur, Kolkata 700032, India and*

⁴ *Solid State and Structural Chemistry Unit, Indian Institute of Science, Bangalore-560012, India*

(Dated: May 8, 2008)

Using first-principles density functional calculations, we study the electronic and magnetic properties of ferromagnetic insulating double-perovskite compound $\text{La}_2\text{NiMnO}_6$, which has been reported to exhibit interesting magnetic field sensitive dielectric anomaly as a function of temperature. Our study reveals existence of very soft infra-red active phonons that couple strongly with spins at the Ni and Mn sites through modification of the super-exchange interaction. We suggest that these modes are the origin for observed dielectric anomaly in $\text{La}_2\text{NiMnO}_6$.

PACS numbers: 71.20.-b, 75.30.Et, 71.45.Gm

Double perovskite $\text{La}_2\text{NiMnO}_6$ (LNMO) is an interesting compound which is a ferromagnetic (FM) insulator with a Curie temperature close to room temperature ($T_c \sim 280$ K). Recently large magnetic field induced changes in dielectric properties have been observed in this compound¹, which makes this compound a promising material for potential device applications². In spite of great technological importance, the theoretical effort for understanding this material is rather limited. To our knowledge, there exists only one report of linear augmented plane wave based basic electronic structure calculations of LNMO, by Matar et al.³.

In this letter, we carried out first-principles density functional calculations to understand the ferromagnetic insulating behavior in this compound as well as to understand the origin of dielectric anomaly that has been observed experimentally¹. We used a combination of two types of methods, namely: (a) muffin-tin orbital based linear muffin-tin orbital⁴ and N-th order muffin-tin orbital (NMTO)⁵ methods, and (b) plane wave-based methods. In the latter, we used ultra-soft pseudopotentials with an energy cutoff of 25 Ry (150 Ry) on the plane wave basis for wave functions (charge density) and a $6 \times 6 \times 6$ mesh of k-points in sampling the Brillouin zone for a phase with unit cell containing one formula unit and equivalent for other phases. In particular, the structural optimization and phonon calculations have been carried out using QUANTUM ESPRESSO⁶ and effective charges and dielectric response have been carried out using ABINIT⁷. The analysis of hopping interactions by constructing effective orbitals, on the other hand, has been carried out within the framework of NMTO. In our LMTO and NMTO calculations, we have used four different empty spheres to achieve the space filling. We used a spin polarized generalized gradient approximation (GGA)⁸ to the exchange correlation functional.

TABLE I: Energy-minimized structural parameters of LNMO. Lattice constants have been kept constant at the experimental values¹¹.

Rhombohedral						
a(Å)	b(Å)	c(Å)		x	y	z
5.474	5.474	5.474	La	0.24980	0.24980	0.24980
α	β	γ	Ni	0.0	0.0	0.0
60.671	60.671	60.671	Mn	0.5	0.5	0.5
			O	0.81403	0.67182	0.25889
Monoclinic						
a(Å)	b(Å)	c(Å)		x	y	z
5.467	5.510	7.751	La	0.00838	0.03781	0.24968
α	β	γ	Ni	0.0	0.5	0.0
			Mn	0.5	0.0	0.0
90.000	90.119	90.000	O1	0.22344	0.20903	0.04140
			O2	0.29189	0.27756	0.45700
			O3	0.42219	0.01454	0.24243

LNMO, having the general structure of a double ordered perovskite ($\text{A}_2\text{BB}'\text{O}_6$), is distorted from the ideal double perovskite, and the amount of distortion changes as the temperature varies. The structure of $\text{La}_2\text{NiMnO}_6$ is rhombohedral ($\text{R}\bar{3}$) at high temperature and transforms to monoclinic ($\text{P}2_1/\text{n}$) at low temperature, with these two structures coexisting over a wide temperature range^{9,10}. In view of the fact that the positions of light atoms are often not well characterized within the experimental technique, we have carried out structural optimization of both rhombohedral (RH) and monoclinic (MC) phases where the internal degrees of freedom associated with La and O atoms have been optimized keeping the lattice parameters fixed at experimentally determined values⁹. The relaxed structural parameters of the rhombohedral FM state (see Table I) agree well within 3 % with experimental ones proving the reliability of our calculation scheme. The position of oxygen atoms, in

*Corresponding Author: tanusri@bose.res.in

particular, the x co-ordinate of O3 oxygen of the MC phase, however differ noticeably (a deviation of about 22 %) from the experimental values (compared Table 3 in ref⁹). Our results may provide basis to further refinement of the experimental structure. Each NiO₆ octahedra in the rhombohedral phase is tilted with respect to MnO₆ octahedra giving rise to Ni-O-Mn bond angle of 157°. The tilting is further increased by 2° in the monoclinic phase. We determined the electronic structure of geometry optimized FM LNMO, for rhombohedral and monoclinic phases using the LMTO⁴ basis, as well as using the plane wave basis⁶. Both methods resulted in similar features in the computed density of states and band structures, and insulating solutions for both RH and MC phases. The spin resolved partial density of states (DOS) of LNMO in the rhombohedral phase, calculated using ESPRESSO, is shown in upper panel of Fig.1. Below -2 eV the predominant contribution is from O-2p states. The octahedral surrounding of Mn and Ni atoms split the Mn and Ni d-manifolds into *t*_{2g} and *e*_g levels. In the up spin channel, the Ni-*t*_{2g} and Ni-*e*_g levels are found in the energy range ~ -2 eV to Fermi energy and show a significant mixing with Mn-d states and O-p states. In the down spin channel the Ni-*t*_{2g} bands are located between O-p states and Fermi level, while Ni-*e*_g states lie ~ 1.2 eV above the Fermi level. This correspond to the nominal valence of Ni²⁺ (d⁸: *t*_{2g}⁶*e*_g²). In the up spin channel the Mn-*t*_{2g} bands are localized between Ni-*t*_{2g} and Ni-*e*_g bands and are filled, while the Mn-*e*_g bands are separated by a gap of ~ 2.5 eV from the Mn-*t*_{2g} bands and remains empty. In the down spin channel, both Mn-*t*_{2g} and Mn-*e*_g bands are located above Fermi level in the energy range ~ 1.5 eV to 5 eV. This leads to conclusion that the oxidation state of Mn is nominally 4+ (d³: *t*_{2g}³*e*_g⁰), which agree with the Mn NMR and X-ray absorption spectroscopy results^{12,13}, though disagree with one of neutron diffraction study¹⁰. Our spin-polarized LMTO calculations gave a moment of 3.0 μ_B at the Mn site within a muffin-tin(MT) radius of 1.32 Å, which agree with experimental value of 3.0 μ_B¹. The magnetic moment at the Ni site, for a MT radius of 1.52 Å is found to be 1.43 μ_B, which is less than the experimentally measured value of 1.9 μ_B. The residual moment is found to reside at the oxygen sites giving rise to the total magnetization of 5.0 μ_B in agreement with the experimental value¹. The spin resolved density of states in the monoclinic structure is shown in the lower panel of Fig.1. The basic nature of DOS is similar to that of rhombohedral phase of LNMO. The occupation of the Ni-d states and Mn-d states suggests again the nominal oxidation states of Ni and Mn ions to be 2+ and 4+, respectively. The moments are found to be 2.91 μ_B within a MT radius of 1.38 Å at the Mn site, 1.35 μ_B at the Ni site within a MT sphere of radius 1.52 Å, and ~ 0.10 μ_B (for 0.95 Å MT radius) at the oxygen site, giving rise to ~ 5.0/f.u total magnetic moment, which is again in agreement with the experimental findings.

LNMO being an insulator, the ferromagnetism in this

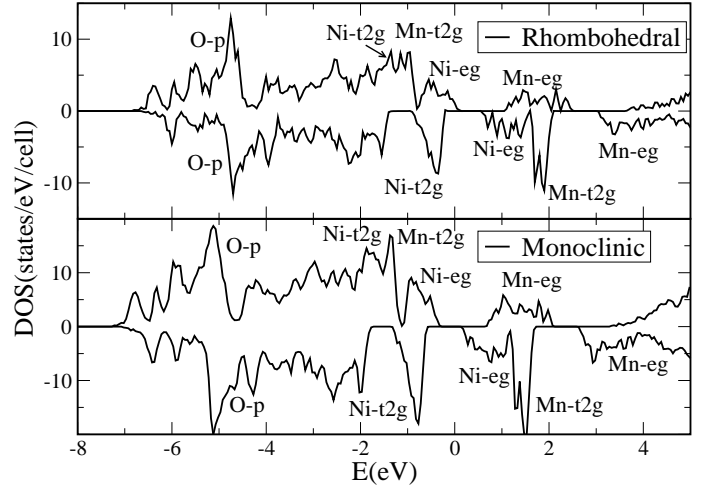


FIG. 1: GGA DOS of LNMO in geometry optimized rhombohedral and monoclinic phases. Zero of the energy is set at the GGA Fermi energy.

compound is expected to be dominated by the localized super-exchange kind of interaction, resulting from the interaction of the half-filled *d* orbital of one metal ion with the vacant *d* orbital of another metal ion through anion *p* orbital. In the following, we show the feasibility of such a scenario by considering the calculated hopping interactions between effective Ni-*d* orbitals and Mn-*d* orbitals. The construction of effective Ni- and Mn-*d* orbitals have been carried out with NMTO- downfolding procedure, by integrating out O and La orbital degrees of freedom and keeping active only the Mn- and Ni-*d* degrees of freedom. This procedure generates the effective Ni- and Mn-*d* orbitals (see Fig. 2) which takes into account the renormalization from the integrated-out oxygen and also La degrees of freedom. Considering an extended Kugel-Khomskii model¹⁴ that includes the hybridization between half-filled Ni *e*_g orbitals and vacant Mn *e*_g orbitals, the virtual hopping of parallelly aligned spins is allowed and is favored over the virtual hopping of antiparallelly aligned spins due to the energy gain via the Hund's coupling J_H . The net exchange can be expressed in terms of the sum of the square of the Ni *e*_g-Mn *e*_g hopping interactions, $\sum_{m,m'} (t_{e^m, e^{m'}})^2$, the onsite energy differences $\Delta_{e,e}$, the onsite Coulomb U and the Hund's coupling J_H as:

$$J_{Ni-Mn}^{(1)} = -4 \frac{\sum_{m,m'} (t_{e^m, e^{m'}})^2 J_H}{(U + \Delta_{e,e} - J_H)(U + \Delta_{e,e})} \quad (1)$$

Considering the hoppings, and onsite energy differences for Ni-Mn neighbors, $\sum_{m,m'} (t_{e^m, e^{m'}})^2$ turns out to be about 0.2 eV while $\Delta_{e,e}$ turns out to be about 1.9 eV. Considering a typical U value of 4 eV and J_H of 0.9 eV, it gives rise to a value of about -24.5 meV for the FM exchange interaction between Ni and Mn.

However, the Ni-Mn exchange interaction has contri-

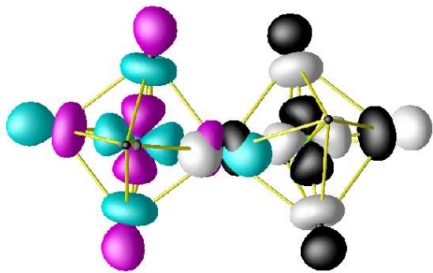


FIG. 2: (Color on-line) Overlap between effective $x^2 - y^2$ orbitals, placed at neighboring NiO_6 and MnO_6 octahedra of LNMO calculated in the monoclinic phase, showing the super-exchange path mediated by the corner-shared oxygen. Plotted are the orbital shapes (constant-amplitude surfaces) with lobes of opposite signs colored as black(magenta) and white(cyan) respectively for Mn(Ni).

bution also from the interaction between half-filled Ni e_g orbitals and Mn t_{2g} orbitals, which should be antiferromagnetic (AFM) in nature, given by:

$$J_{\text{Ni-Mn}}^{(2)} = 4 \frac{\sum_{m,m'} (t_{e^m, t^{m'}})^2}{(U + \Delta_{e,t})} \quad (2)$$

The summation m, m' in the above runs over half-filled e_g and t_{2g} orbitals at Ni and Mn sites, respectively. The computed sum of squares of the Ni e_g -Mn t_{2g} hopping interactions in the basis of NMTO-Wannier functions turns out to be about 0.02 eV, while the on-site energy difference turns out to be about 0.25 eV. Putting these values in Eqn.(2) it gives rise to a value of about 19 meV for $J^{(2)}$. The net exchange interaction, therefore, comes out to be ferromagnetic with a value of about 5 meV¹⁵, which is a reasonable estimate considering the rather approximate nature of the perturbative approach. The mean-field T_c computed with this estimate of Ni-Mn exchange interaction comes out to be 350 K compared to experimental estimate of 280 K¹⁶.

In the following, we investigate the origin of magnetocapacitance in LNMO manifested in the dielectric anomaly¹ as a function of magnetic field. The dielectric constant of LNMO is known¹ to increase with temperature and exhibit a jump at T_{jump} . T_{jump} depends sensitively on magnetic field, particularly for small fields (≤ 0.1 T). Since the electronic contribution to dielectric constant of insulators such as LNMO is typically much smaller¹⁷ than the magnitude of jump in the dielectric constant, we expect the origin of this coupling between magnetic field and dielectric response to emerge from the couplings between spin and structure, *i.e.*, phonons.

To determine the coupling between spin and various phonons, we studied the response of optimized FM rhombohedral structure to changes in magnetic ordering: *e.g.* changes in phonon frequencies with changes in magnetic

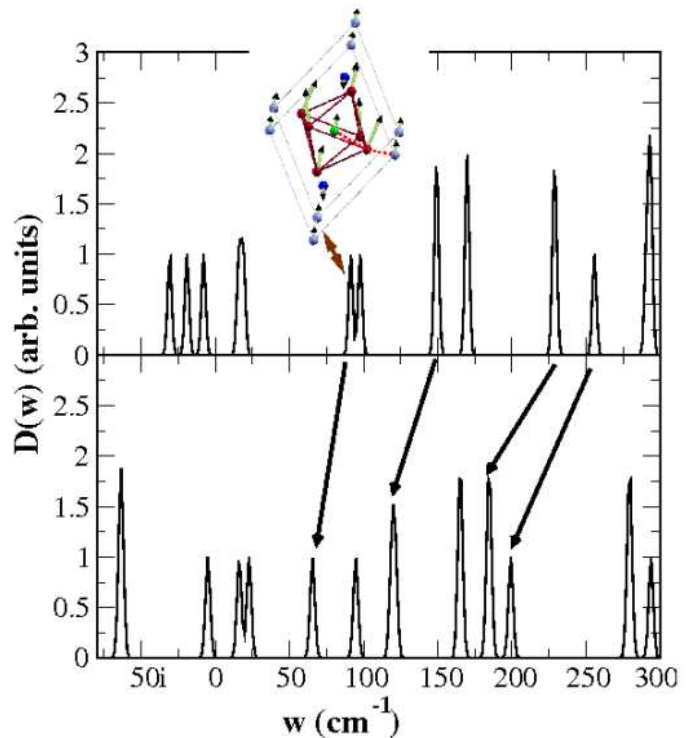


FIG. 3: (Color online) Phonon spectra of rhombohedral LNMO in FM (top panel) and FIM (bottom panel) states. The arrows show the shifting of dominant IR active phonon modes. The inset shows the displacement of atoms corresponding to the lowest frequency IR-active mode. The angle between the red dotted lines connecting the Ni(at the center of the oxygen-octahedra)-O and O-Mn (rightmost corner of the cell) is affected by this phonon.

ordering. We determined changes in phonon frequencies upon changing the neighboring spin to antiparallel, the so called Ferrimagnetic (FIM) alignment. Note that any other different spin arrangement other than FM spin arrangement would have been equally qualified for this purpose. The charge states of Ni and Mn in the FIM state are found to remain same as that in the FM state. Hellman-Feynman forces acting on atoms in the FIM phase, give us the lowest order coupling between spins and phonons which is linear in atomic displacements. We find that these forces are equal and opposite for pairs of atoms, hence this coupling is zero for any IR-active modes and should have no direct implications to the observed dielectric anomaly. Next, we determined the Γ -point phonons for the rhombohedral structure with FM and FIM ordering. Shifts in the phonon frequencies give the coupling between spins and atomic displacements at the second order. Since the rhombohedral structure is unstable at $T=0$ K, we find two marginally unstable modes ($31i$ and $19i$ cm^{-1}) which are IR-inactive and couple strongly with spins: their frequencies change to $64i$ and $63i$ cm^{-1} in the FIM phase. We find that frequencies

of the lowest energy IR-active phonons soften from 91.3, 149, 228 and 255 cm^{-1} in the FM phase to 65.5, 120, 184 and 199 cm^{-1} respectively (indicated by arrows in Fig.3), exhibiting a strong coupling with spin. This may be compared with the recently studied case of CdCr_2S_4 ¹⁸ where the significant polar mode was found only at frequency of 300 cm^{-1} . This results in change in static dielectric constant from 119 in FM state to 221 in the FIM state, which is dominated by the softest IR-active mode (see inset of Fig.3) with a contribution of 77 and 185, respectively. Atomic displacements in this softest mode, are such that they would make the Ni-O-Mn angles closer to 180° , in an average sense, leading to enhancement of the superexchange interaction. The decrease in phonon frequency for the spin-paired Ni-Mn in FIM phase compared to spin-antipaired Ni-Mn in FM phase can be explained by analyzing the spin Hamiltonian $\text{JS}_i \cdot \text{S}_j$ and noting that the magnetic super-exchange coupling J depends on $\angle \text{Ni-O-Mn}$, θ , as $\cos^2(\theta)$. Expanding $\cos^2(\theta)$, about the equilibrium value of $\angle \text{Ni-O-Mn}$, $\theta_0 \approx 157^\circ$, and assuming $\theta = \theta_0 + u$, u being the displacement, the spin-phonon coupling turns out to be positive for the term linear in u and negative for the term quadratic in u . The latter effectively gives a positive change in phonon frequency due to the additional negative sign, associated with FM nature of the magnetic interaction (cf. Eqn.1).

To conclude, we carried out first principles DFT calculations to examine the electronic and magnetic structure

of $\text{La}_2\text{NiMnO}_6$, in particular, to understand the origin of the dielectric anomaly reported recently. We could correctly reproduce the ferromagnetic insulating behavior of the compound, the ferromagnetism being governed by the super-exchange interaction. Our study further showed presence of soft IR-active phonon modes exhibiting strong coupling with spin, which explains the observed dielectric anomaly. The fact that the jump in the dielectric constant at $H=0$ T, occurs at a temperature T_{jump} below T_c happens because close to T_c the magnetic moment is not fully developed due to thermal fluctuation while at lower temperature the moment gets fully developed and makes the effect of coupling to phonon degrees of freedom appreciable enough to observe the jump in dielectric constant. This is corroborated by the fact that T_{jump} becomes closer to T_c upon application of magnetic field, which helps overcoming the thermal fluctuation and enhance the magnetization. Note that superexchange driven B-site magnetism based dielectric anomaly discussed here is complementary to the mechanism of the low-temperature dielectric anomaly discussed for EuTiO_3 ¹⁹, which is A-site based weak magnetism driven.

Acknowledgment- T.S.-D and D.D.S acknowledge support of Swarnajayanti and J.C.Bose grants. U.V.W. thanks SNBose Centre for hospitality during the execution of the work and CCMS at JNCASR for partial support.

-
- ¹ Nyrissa S. Rogado, Jun Li, Arthur W. Sleight, and Mas A. Subramanian, *Adv. Mater.* **17**, 2225 (2005).
- ² M. Hashisaka, D. Kan, A. Masuno, T. Terashima, M. Takano and K. Mibu, *Journal of Magnetism and Magnetic Materials* **310**, 1975 (2007); H. Guo *et al.* *Appl. Phys. Lett.* **89**, 022509 (2006).
- ³ S. F. Matar, M. A. Subramanian, V. Eyert, M. Whangbo and A. Villesuzanne (unpublished).
- ⁴ O. K. Andersen, *Phys. Rev. B*, **12**(1975) 3060.
- ⁵ O. K. Andersen and T. Saha-Dasgupta, *Phys. Rev. B* **62**, R16219(2000).
- ⁶ S. Baroni *et. al.* <http://www.pwscf.org/>.
- ⁷ Gonze *et. al.* <http://www.abinit.org/>.
- ⁸ J. P. Perdew, K. Burke, and M. Ernzerhof, *Phys. Rev. Lett.* **77**, 3865 (1996).
- ⁹ C. L. Bull, D. Gleeson, K. S. Knight, *J. Phys. Condens. Matter* **15**, 4927 (2003).
- ¹⁰ K. Asai *et. al.* *J. Phys. Soc. Jpn.* **47**, 1054 (1979).
- ¹¹ We have also carried out volume optimization of the crystal structure both for RH and monoclinic phases. The GGA theoretical lattice parameters are very close to the experimental estimates [by less than 0.5%]: 5.537 Å and 5.478 Å instead of experimental estimates of 5.510 Å and 5.474 Å for monoclinic and RH phases respectively. The structural co-ordinates change at the most by 0.2% for the monoclinic phase and less than 0.1% for the RH phase.
- ¹² M. Sonobe, K. Asai, *J. Phys. Soc. Jpn.* **61**, 4193 (1992).
- ¹³ M. C. Sanchez *et. al.* *Phys. Rev. B* **65**, 144 409 (2002).
- ¹⁴ K. I. Kugel and D. I. Khomskii, *Sov. Phys. Usp.* **25** 231 (1982).
- ¹⁵ In this simplistic formulation, we have assumed that the value of U and J_H to be the same between Ni and Mn. While J_H is fairly constant between different elements, U can vary. Mn is expected to have a smaller U value than Ni. Considering a U value of 3 eV for Mn and 5 eV for Ni, one gets an average U value of 4 eV. Changing U by 5 to 10%, we find that the calculated effective J turn out to be having a value between 4 - 7 meV.
- ¹⁶ We also attempted to extract the net magnetic coupling, J , by taking the total energy difference between FM and FIM configuration of Ni and Mn spins. LDA total energy differences are however known to overestimate the value of J due to LDA overbinding problem. Our computed J turned out to be about 14 meV, which overestimate the perturbatively computed J by a factor of about 3. Introduction of spin-orbit coupling changes the magnitude of J by less than 1%, maintaining the FM nature of J .
- ¹⁷ This is supported by our ab-initio calculation, which gives ϵ^∞ equal to 22 and 20 for two different magnetic phases, namely FM and ferrimagnetic phases.
- ¹⁸ C. J. Fennie and K. M. Rabe, *Phys. Rev. B* **72** 214123 (2005).
- ¹⁹ C. J. Fennie and K. M. Rabe, *Phys. Rev. Lett.* **97**, 267602 (2006).